CELL BIOLOGY

Reciprocal regulation of TORC signaling and tRNA modifications by Elongator enforces nutrient-dependent cell fate

Julie Candiracci[1], Valerie Migeot[1], Yok-Hian Chionh[2]*, Fanelie Bauer[1], Thomas Brochier[1], Brandon Russell[3†], Kazuhiro Shiozaki[4,5], Peter Dedon[2,3], Damien Hermand[1‡]

Nutrient availability has a profound impact on cell fate. Upon nitrogen starvation, wild-type fission yeast cells uncouple cell growth from cell division to generate small, round-shaped cells that are competent for sexual differentiation. The TORC1 (TOR complex 1) and TORC2 complexes exert opposite controls on cell growth and cell differentiation, but little is known about how their activity is coordinated. We show that transfer RNA (tRNA) modifications by Elongator are critical for this regulation by promoting the translation of both key components of TORC2 and repressors of TORC1. We further identified the TORC2 pathway as an activator of Elongator by down-regulating a Gsk3 (glycogen synthase kinase 3)–dependent inhibitory phosphorylation of Elongator. Therefore, a feedback control is operating between TOR complex (TORC) signaling and tRNA modification by Elongator to enforce the advancement of mitosis that precedes cell differentiation.

INTRODUCTION

Fission yeast sexual differentiation has evolved as a stress response, and almost any sudden change in growth conditions induces some cells to accelerate mitosis, become smaller, and enter gametogenesis, even in chemostat cultures (*1*). This is also observed on plated colonies where the heterogeneity of nutrient availability generates regions more or less conducive to differentiation, which is conveniently induced under laboratory conditions by altering, limiting, or withdrawing the source of nitrogen (*2*). More generally, in cultured cells or in whole organisms, the critical cell size for mitosis is determined by the growth conditions (*3*, *4*). TOR (target of rapamycin) signaling is a conserved central mediator of this process. TOR regulates nutrient uptake, gene expression, protein synthesis, and metabolic pathways to ensure that the balance between cell growth and cell division is coordinated with nutrient availability. The process is evolutionarily conserved and notably shown in flies grown under nutrient-limiting conditions that develop to half of the size of well-fed animals without a reduction of the absolute cell number (*3*, *4*). In fission yeast (Fig. 1A), TORC1 (TOR complex 1) defined by the Tor2 kinase and the raptor homolog Mip1 is sensitive to rapamycin, promotes cell growth, and inhibits entry into mitosis while repressing autophagy and cell differentiation. TORC2 defined by the Tor1 kinase and the Rictor homolog Ste20 promotes mitosis and is essential for differentiation (*5–11*). Consequently, TORC1 mutants uncouple nutrient availability from growth and have an "always starved" phenotype. These mutants eventually arrest as small rounded cell even when nitrogen is abundant. In contrast, TORC2 mutants uncouple starvation from gametogenesis and have a "never starved" phenotype resulting in sterility when nitrogen drops. On the basis of genetic analyses and the antagonistic relationship between TORC1 and TORC2, the concept of feedback loops connecting both complexes was suggested early on (*12*) but lacked mechanistic support until recently (*13*, *14*).

Transfer RNAs (tRNAs) from all organisms contain modified nucleosides, and when a uridine is present in the wobble position (U_{34}), this residue is almost universally modified (*15–17*). In particular, the eukaryotic cytosolic $tRNA^{Lys}_{UUU}$ is thiolated (s^2) by the Ctu1 enzyme at the 2-carbon and contains the most critical methoxy-carbonyl-methyl (mcm^5) modification at the 5-carbon on the wobble uridine, which is required to offset the translational inefficiency resulting from low effective stacking interactions of the A-U base interaction (*18–20*). The six-subunit Elongator complex synthetizes the cm^5 moiety, which becomes a substrate for the Trm9 methylase to generate mcm^5U (fig. S1A) (*21–23*). The catalytic subunit of Elongator is Elp3. Two copies of the Elp1-Elp2-Elp3 subunits form a two-lobe symmetric scaffold, which asymmetrically binds Elp4-Elp5-Elp6. In all species where it has been investigated, the absence of any subunits results in the inactivation of the whole complex, and mutants show an extremely diverse range of phenotypes (*24*). In fission yeast, a major phenotype resulting from the inactivation of Elongator is a cell cycle defect, and the *cdr2* mRNA that encodes a key regulator of mitosis and cytokinesis was shown to harbor a skewed codon content for lysine, which places it under translational control by Elongator (*25*, *26*). In the present study, we report a reciprocal regulation of TOR complex (TORC) signaling and Elongator, showing that tRNA modification by Elongator is at the nexus of cell growth and cell differentiation.

RESULTS

Our previous proteome-wide analysis of a fission yeast strain lacking the Elp3 subunit of Elongator revealed that four distinct functional Gene Ontology (GO) groups of proteins were down-regulated (*25–27*). Analysis of the codon usage within the corresponding mRNAs

[1]URPHYM-GEMO, University of Namur, rue de Bruxelles, 61, Namur 5000, Belgium. [2]Singapore–MIT Alliance for Research and Technology Centre (SMART), Center for Life Sciences 05-06, 28 Medical Drive, 117456 Singapore. [3]Massachusetts Institute of Technology, 56-787B77 Massachusetts Avenue, Cambridge, MA 02139-4307, USA. [4]Division of Biological Science, Nara Institute of Science and Technology, Ikoma, Nara 630-0192, Japan. [5]Department of Microbiology and Molecular Genetics, University of California, Davis, CA 95616, USA.
*Present address: Tychan Pte. Ltd., 79 Ayer Rajah Crescent, 05-03, 139955 Singapore.
†Present address: GSK, 5 Moore Drive, Research Triangle Park, NC 27709, USA.
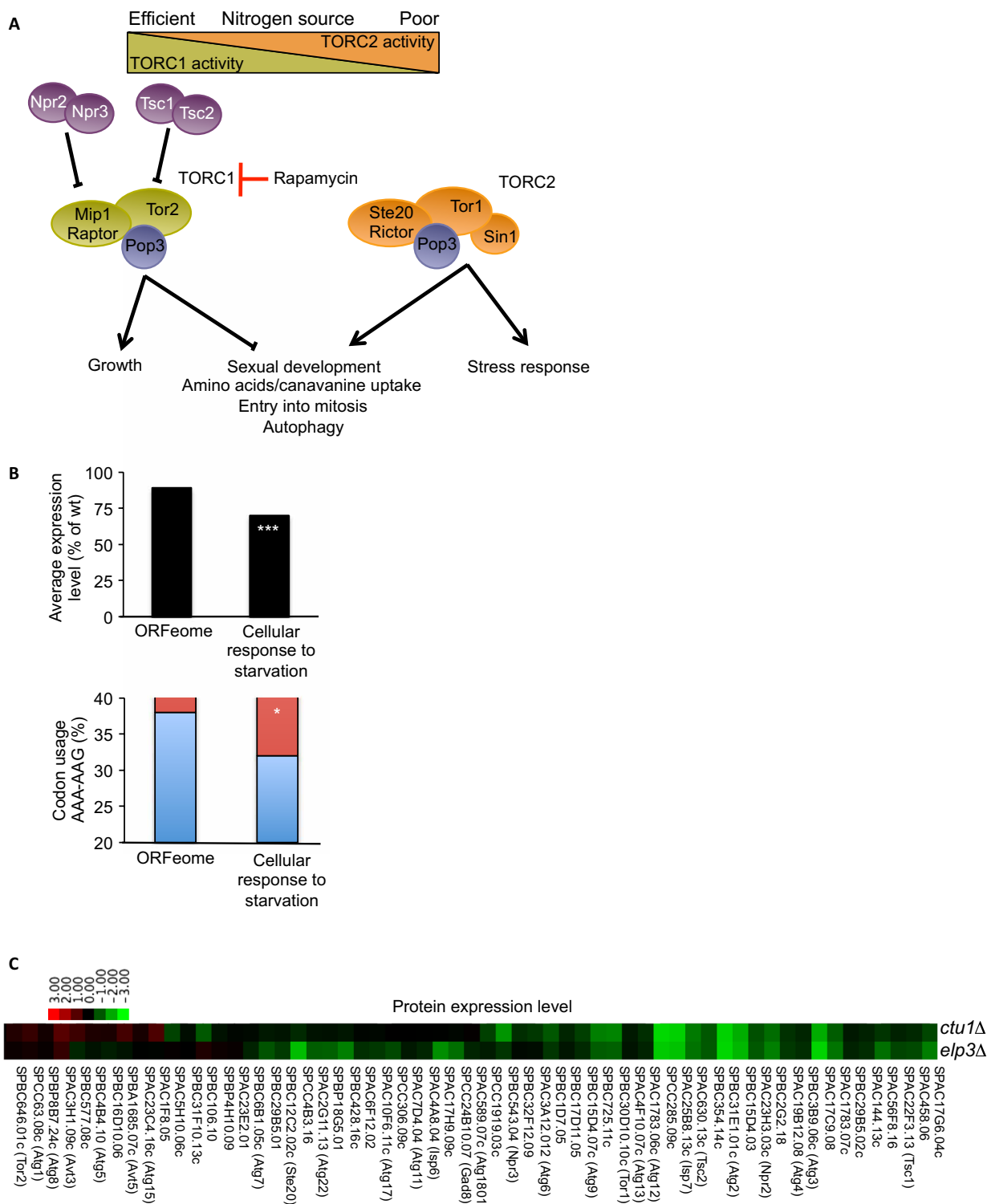‡Corresponding author. Email: damien.hermand@unamur.be

Fig. 1. The Elongator complex regulates the expression of components of TORC1/TORC2 signaling pathways. (**A**) A schematic of the TORC1 and TORC2 signaling pathways in fission yeast. The quality and availability of the nitrogen source control the balance between TORC1 that enforces growth and TORC2 that enforces cell differentiation. (**B**) Top: Average expression level of the proteome in the *elp3*-deleted strain compared to wild type set to 100%. Average expression level within the GO functional group (cellular response to starvation) was significantly more affected than the average in the absence of Elongator (*$P < 0.05$; **$P < 0.01$; Student's t test). Bottom: Codon usage for lysine (AAA-AAG), within the GO functional group (cellular response to starvation) compared to the average ORFeome lysine (AAA-AAG) codon usage. Note that the 0 to 20% and 40 to 100% of the y axis are not shown to highlight variations from the ORFeome codon usage. (*$P < 0.05$; **$P < 0.01$; ***$P < 0.001$; Student's t test). wt, wild type. (**C**) Hierarchical clustering and heat map analysis of the expression level within the GO functional group (cellular response to starvation) in the *ctu1* and *elp3* deletion strains compared to wild type. The data are presented as log 2 mutant/wild-type ratio of immunoblotting signals and are color-coded as indicated in the key.

showed a bias for the AAA codon over AAG when encoding lysine, which rendered their expression highly dependent on the modification by Elongator (*26*). A detailed analysis of one GO group related to the response to nutrients and the TOR signaling pathway highlighted the presence of many autophagy-dependent (Atg) proteins, with autophagy controlled by the TOR pathway (Fig. 1B). In addition,

the expression of positive effectors of TORC2 (Tor1, Ste20[Rictor], and Gad8) and inhibitors of TORC1 (Tsc1, Tsc2, Npr2, and Npr3) was also down-regulated in the absence of Elp3 (Fig. 1C and fig. S1B). The overexpression of the unmodified $tRNA^{LYS}_{UUU}$ was sufficient to restore wild-type level of Ste20[Rictor] and Tsc2 (Fig. 2A) while suppressing the rapamycin sensitivity of the *elp3* mutant (Fig. 2B),
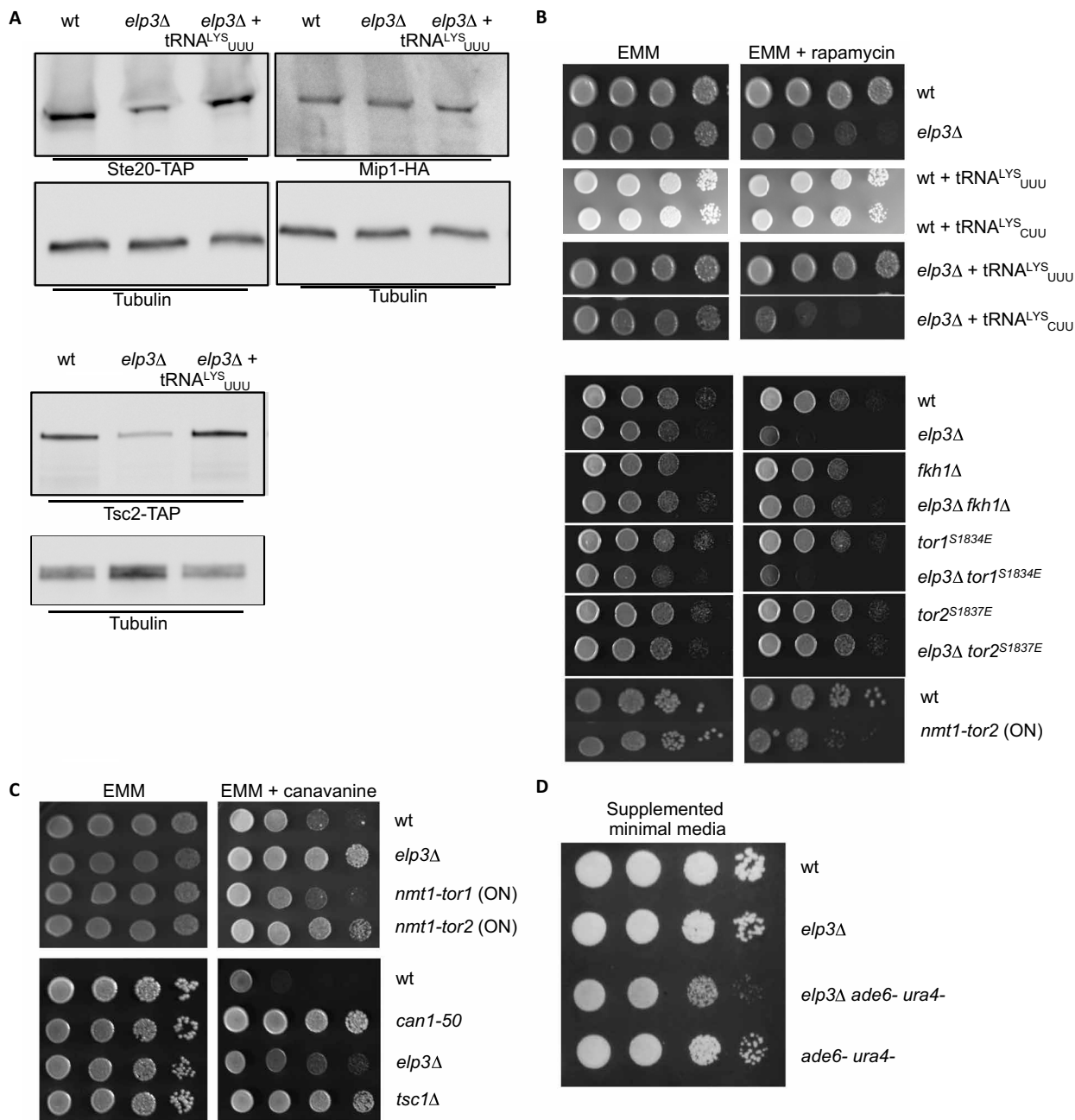

Fig. 2. The Elongator complex regulates the balance between TORC1 and TORC2 activities. (**A**) Western blot analysis of the level of expression of Ste20-TAP (Tandem Affinity Purification) (Rictor in TORC1), Mip1-HA (Raptor in TORC2), and Tsc2 in the indicated strains showing the specific down-regulation of Ste20 and Tsc2 when Elongator is inactivated and the rescue when the $tRNA^{LYS}_{UUU}$ is overexpressed. Tubulin is used as a loading control. (**B**) Growth assay of the indicated strains in the presence or absence of rapamycin. The *tor1 S1834E* and *tor2 S1837E* are rapamycin-resistant alleles. *nmt1-tor2* is overexpressing the genes from the *nmt1* promoter. EMM, Edinburgh minimal medium. (**C**) Growth assay of the indicated strains in the presence or absence of canavanine. The *can1-50* allele harbors a mutation of the canavanine transporter Can1, resulting in resistance. *nmt1-tor1* and *nmt1-tor2* are overexpressing the genes from the *nmt1* promoter. (**D**) Growth assay of the indicated prototrophic or auxotrophic strains grown on minimal media supplemented with adenine and uracil.

supporting a close connection bewteen Elongator and the TORC1/TORC2 pathways. A broader phenotypic analysis showed that the sensitivity of the *elp3* mutant to rapamycin was mediated through the Fkh1 protein and through the TORC1 complex, as a rapamycin-resistant *tor2* allele (*tor2 S1873E*) completely suppressed the sensitivity while the corresponding rapamycin-resistant *tor1* allele (*tor1 S1834E*) did not (Fig. 2B). This set of data suggested that the sensitivity of Elongator mutants to rapamycin resulted from the increased activity of TORC1 and unbalanced TORC signaling, as supported by the fact that the overexpression of *tor2* also increased the sensitivity to rapamycin (Fig. 2B). In addition, the absence of Elongator resulted in resistance to canavanine (Fig. 2C), similar to the overexpression of *tor2*, or the deletion of *tsc1*, a gene encoding hamartin that negatively regulates TORC1 (Fig. 2C). Auxothrophic *elp3* mutants grew poorly on supplemented minimal media, suggesting a deficient nutrient uptake that is also typical of unbalanced TOR signaling in benefit of TORC1 (Fig. 2D). Together, these results support that Elongator acts as a positive regulator of TORC2 and a negative regulator of TORC1 through translational controls of components of these complexes and may therefore regulate the balance between both complexes.

To test this possibility, we analyzed the behavior of the Elongator mutant during nutrient shifts between efficient (glutamate) and poor (proline) nitrogen sources, which alters the TORC1/TORC2 balance (*28–30*). Wild-type cells shifted from glutamate to proline were advanced into mitosis, as shown by a peak in the percentage of dividing cells about 1 hour after the nutritional shift (Fig. 3A). The proportion of dividing cells remained largely constant in an Elongator mutant (*elp4* deletion), indicating that the advancement into mitosis was not efficient when Elongator was inactivated. Rapamycin was previously shown to mimic the nutritional shift-down (*30*). The use of rapamycin-resistant versions of *tor1* and *tor2* indicated that the mitotic advancement likely occurred by inhibiting TORC1 for the benefit of TORC2, as rapamycin had no effect on a strain harboring the rapamycin-resistant *tor2 S1837E* allele (Fig. 3B). In the reverse experiment where cells were shifted from the poor nitrogen source proline to glutamate, a drop in the percentage of dividing cells was observed within 1 hour, indicating a delayed onset of mitosis, which restores TORC1-dependent promotion of growth. While the *elp4* mutant barely affected this response, cells remained delayed about 30 min longer, suggesting TORC1 hyperactivation (Fig. 3C). These data support the possibility that the Elongator complex is a critical regulator of the balance between the TORC1 and TORC2 complexes when environmental cues controlling the commitment to mitosis are changing.

To identify regulators of the activity of Elongator, we next set up a genetic screen based on dual-color luciferase reporters harboring skewed codon content for lysine. We generated a strain expressing the green-emitting click beetle luciferase (CBG) expressed from the *ura4* locus and the red-emitting click beetle luciferase (CBR) expressed from the *leu1* locus (*31*), which is suitable for Chroma-Glo assays carried out directly in the culture medium (fig. S2A). The natural codon bias for lysine (CBR: 35% Lys^{AAA}/65% Lys^{AAG} and CBG: 54% Lys^{AAA}/46% Lys^{AAG}) was sufficient to render their expression sensitive to the absence of Elongator, with CBG being the most affected. However, CBR was also affected and therefore was not suitable as internal control. We therefore modified the reporter strain by using a CBG$_{AAG}$ version, where all lysine codons are encoded by the AAG codon, and a CBR$_{AAA}$ version, where all lysine codons are encoded by the AAA codon. In addition, CBG$_{AAG}$ was fused to the Ade3 protein, which we have shown to be expressed independently of Elongator, and CBR$_{AAA}$ was fused to the Cdr2 protein, which we have shown to require Elongator for efficient translation (*26*). Both reporters were stably expressed, and the steady-state levels of their mRNAs were independent of the *elp3*, *ctu1*, and *trm9* genes required for the synthesis of the mcm^{5}s^{2}U modification, while the bio-luminescence of CBR$_{AAA}$, but not CBG$_{AAG}$, was affected in the absence of these three genes (fig. S2, B to D). The reporter strain was crossed to the fission yeast deletion library, and the resulting strains were screened for altered dual-color luminescence ratio (fig. S3A). An increased or decreased CBR/CBG ratio was found in 417 clones, suggesting that the translation of the reporter of Elongator activity can be either up- or down-regulated (table S1). Considering this large number of candidates and the possibility of cell cycle effects resulting from using the Cdr2 fusion, the positive clones were screened for altered expression of Atf1, another well-characterized but unrelated target of Elongator (*32*). The set of 100 clones that behaved similarly in both screens was further analyzed. We found that the *tsc1*, *tor1*, and *ekc1* genes encoding key players of the TOR pathways were recovered in both screens, and this list was further extended to *tsc2*, *npr2*, *ste20*, and *hhp2* when considering only screen 1 (fig. S3B). The casein kinase Hhp2 (Hrr25) and the Ekc1 (Sit4) phosphatase subunit were previously shown to be required for the activity of Elongator in budding yeast (fig. S3C) (*23*, *33*), further validating the screens. The fact that inhibitors of TORC1 (Tsc1, Tsc2, and Npr2) and components of TORC2 (Tor1 and Ste20) were identified as positive regulators of Elongator suggested that, while Elongator is required for proper balance between TORC1 and TORC2, TORCs could in turn regulate the synthesis of the modification by Elongator (fig. S3C).

To explore this possibility, we first adapted the previously described liquid chromatography–coupled mass spectrometry (LC-MS) quantitative approach (*34*) to fission yeast. Analysis of the *elp3* and *ctu1* single mutants and the double *elp3*/*ctu1* mutant confirmed our previous work (*35*) showing the loss of canonical Elongator-dependent modifications in the absence of *elp3* and the specific loss of s^2 when *ctu1* is deleted, while a set of unrelated modifications was barely affected (Fig. 4A). We next focused on the complete set of detectable modified nucleosides dependent on Elongator activity (fig. S1A) and analyzed them in strains overexpressing either *tor1* or *tor2* or grown in the presence of rapamycin. This experiment revealed that the inhibition of TORC1 by rapamycin or the overexpression of the TORC2 kinase Tor1 resulted in an increase in the cm^{5}U and cm^{5}Um nucleotides, while the overexpression of the TORC1 kinase Tor2 had the opposite effect (Fig. 4A and fig. S4, A to C). These data indicate that the artificial manipulation of TOR signaling affects the level of the Elongator-dependent modifications, with TORC1 and TORC2 showing an opposite effect. The increased levels of cm^{5}U or cm^{5}Um are reminiscent of the deletion of *trm9*, suggesting that the methylase may become limiting when Elongator activity is increased.

Phosphoproteome-wide analyses in budding yeast have highlighted that the Elp4 subunit of Elongator undergoes rapamycin-dependent phosphorylation on serine-221 (*36*). The same region in fission yeast Elp4 (fig. S5A) was reported to be phosphorylated in two independent large-scale analyses (*37*, *38*). In this latter case, the targeted sites are S114 and S118 in the S^{114}S^{115}P^{116}P^{117}S^{118} sequence, which are conserved within the fission yeast clade (fig. S5B). In addition, the
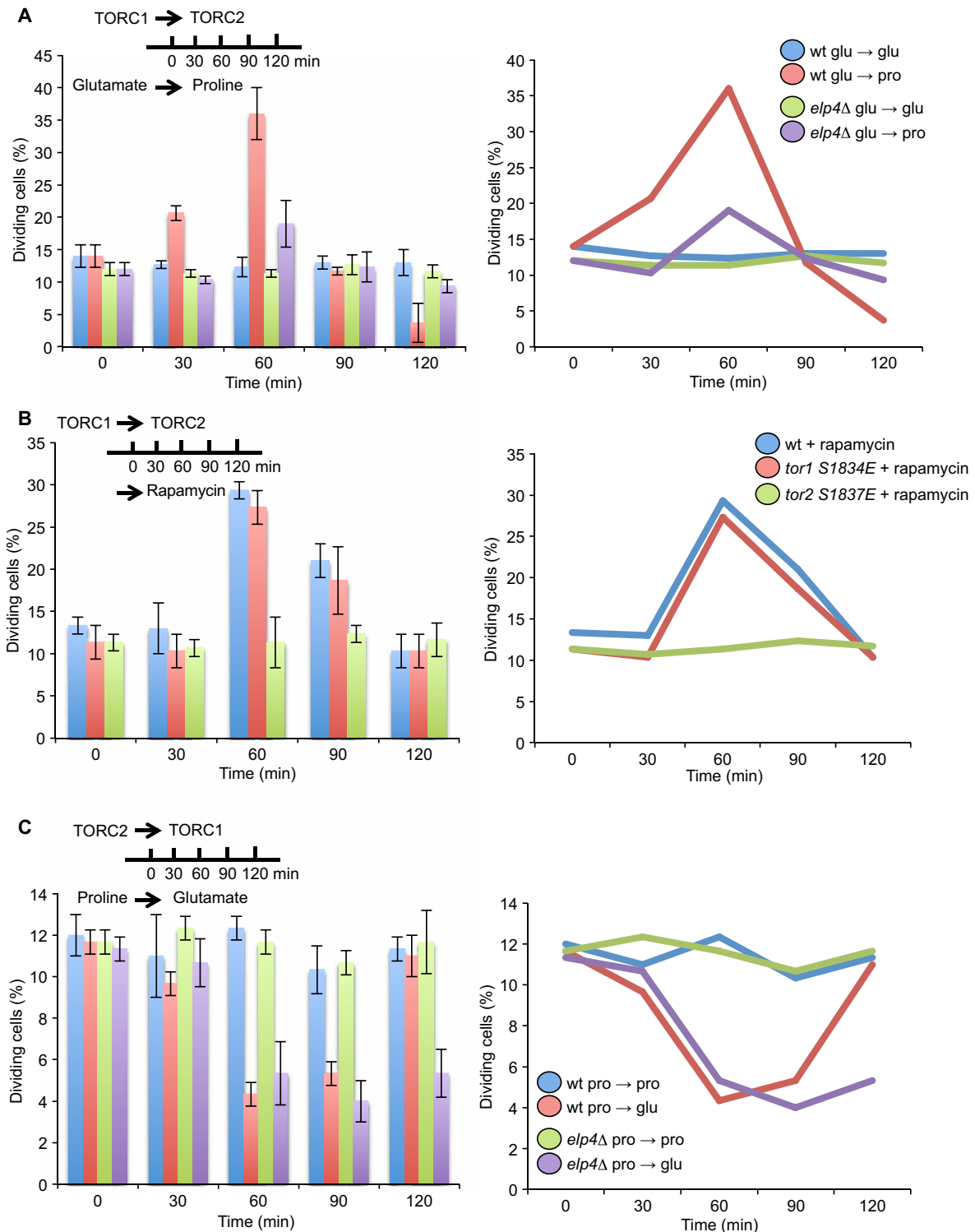
Fig. 3. The Elongator complex is required for the nutrient-dependent shift between the TORC1 and TORC2 complexes. (**A**) The percentage of dividing cells was determined during a shift from an efficient (glutamate) and a poor (proline) nitrogen source in wild-type or Elongator-deficient strains. A glutamate-to-glutamate shift is shown as control. Each column represents the averaged value ± SEM (n = 3). Right: Averaged values for clarity. Note that an *elp4* mutant was used, as Elp4 will be the focus of the rest of the manuscript, but that the deletion of any subunit of Elongator results in the inactivation of the whole complex. (**B**) The percentage of dividing cells was determined after addition of rapamycin that mimics the mitotic advancement following a nutritional shift. The indicated strains including rapamycin-resistant alleles of *tor1* and *tor2* were used. Each column represents the averaged value ± SEM (n = 3). Right: Averaged values for clarity. (**C**) The percentage of dividing cells was determined after a shift from a poor (proline) to an efficient (glutamate) nitrogen source in wild-type or Elongator-deficient strains. A proline-to-proline shift is shown as control. Each column represents the averaged value ± SEM (n = 3). Right: Averaged values for clarity.
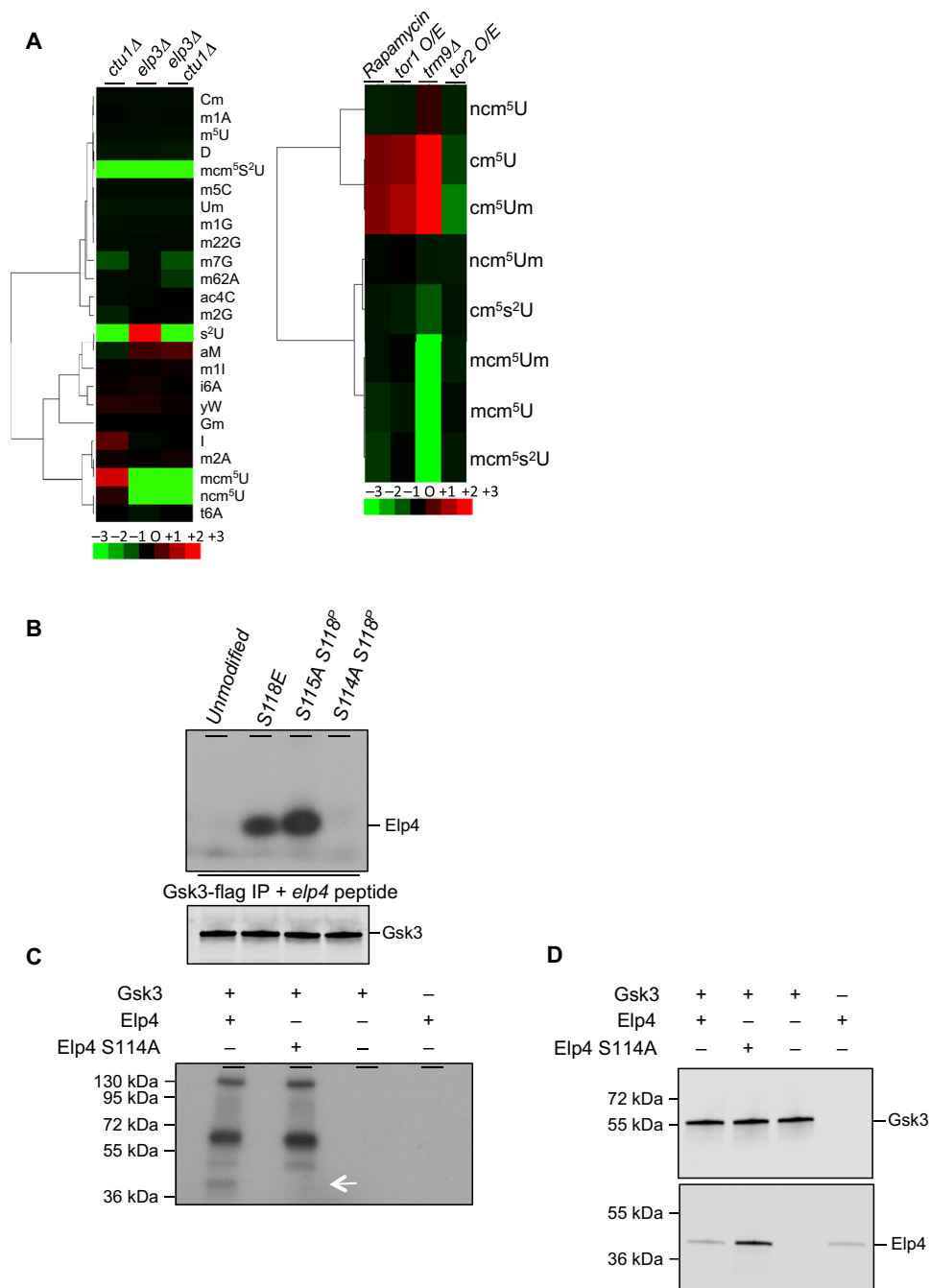
Fig. 4. The TORC1/TORC2 pathway controls the level of the Elongator-dependent modifications. (**A**) Left: Hierachical clustering analysis of changes in the relative levels of a set of tRNA ribonucleoside modifications in mutants of genes required for the synthesis of wobble s^2 (*ctu1*) and mcm^5 (*elp3*) uridine moieties. The bottom color bar displays the range of log 2 fold change values. Right: Similar to that in the left, except that all detectable Elongator-dependent modified ribonucleosides are shown and the following conditions were applied: treatment with rapamycin, overexpression of *tor1* or *tor2*, deletion of the *trm9* gene encoding the enzyme required for the methylation of the cm^5 moiety of the mcm^5U and mcm^5s^2U modifications. (**B**) Phosphorylation assay of peptides corresponding to the amino acids 107 to 120 of fission yeast Elp4 harboring the indicated mutations or phosphorylation (*S118^P*) using immunoprecipitated Gsk3-flag. (**C**) Phosphorylation assay of endogenous immunoprecipitated Elp4-TAP protein (wt or S114A as indicated) mixed with immunoprecipitated Gsk3-flag before the kinase assay. The band corresponding to Elp4 (40 kDa) is indicated by an arrow. (**D**) Western blot controlling the level of Gsk3 or Elp4 from the experiment shown in (C). Half of the immunoprecipitation (IP) products were used. Note that the Elp4 S114A mutant is expressed at higher level (see below).

deletion of the *elp4* gene in *Schizosaccharomyces japonicus* also resulted in increased sensitivity to rapamycin, which supports a conservation of the TOR-Elongator connection (fig. S5C). Serine-114 constitutes a glycogen synthase kinase 3 (Gsk3) consensus site, as this kinase requires a priming phosphorylation at the +4 residue. These findings were of interest, as Gsk3 is known to be negatively regulated by the Akt kinase downstream of the TORC pathway (*39*, *40*).

We first tested the ability of Gsk3 to phosphorylate an Elp4 peptide encompassing the targeted region. Immunoprecipitated Gsk3 only phosphorylated the Elp4 peptide prephosphorylated at position 118 and harboring a serine at position 114, which confirmed the dependency of Gsk3 for a priming phosphorylation at +4 (Fig. 4B). To test the ability of Gsk3 to phosphorylate the endogenous Elp4, we precipitated Gsk3 and Elp4 from fission yeast cells and mixed the precipitated products for a subsequent kinase assay. Gsk3 phosphorylated multiple proteins from the Elp4 immunoprecipitation (IP), with one band fully dependent on the presence of a serine at position 114 on Elp4 (Fig. 4, C and D). Together, these data strongly support that Elp4 is a target of Gsk3 in fission yeast.

We next confirmed that the fission yeast Akt kinase Gad8 phosphorylated the fission yeast Gsk3 in vitro using a recombinant glutathione *S*-transferase (GST)–Gsk3 as a substrate. A previous study had identified S335 as a major, albeit not unique, inhibitory phosphorylated site (*41*), and the phosphorylation of Gsk3 by Gad8 was indeed reduced when a GST-Gsk3 S335A protein was used as a substrate (fig. S6, A to C). These data supported a conservation of the TOR → Akt → Gsk3 connection in fission yeast. Moreover, recombinant GST-Gsk3 harboring a S335E mutation was less active than the wild-type version (fig. S6D). In addition, the activity of Gsk3 on Elp4 was increased in a *gad8* mutant (fig. S6D) and strongly decreased when nitrogen was removed (fig. S6E), a condition known to activate the TORC2-Gad8 branch of the TOR pathway. Despite the fact that, in this case, the level of the Gsk3 protein dropped, the expected net consequence is a decreased phosphorylation of Elp4 on S114.

To analyze the consequence of Elp4 phosphorylation, we generated unphosphorylatable and phospho-mimic S114 and S118 versions of Elp4 and examined their phenotypes. As an intermediate step in creating the *elp4* mutant, we generated a strain disrupted for *elp4* by retaining only the first 91 amino acids. Unexpectedly, this truncated version behaved as a dominant negative, as the expression of wild-type *elp4* could not fully complement the rapamycin sensitivity of the strain (Fig. 5, A and B). The S114A mutant grew much better than the wild type, bypassing the dominant-negative phenotype, which suggested that the S114 phosphorylation by Gsk3 is inhibitory and that its removal in the S114A mutant generates a hyperactive version of Elongator. In contrast, mutating S114, the phospho-mimic glutamic acid, decreased the ability of the strain to grow in the presence of rapamycin (Fig. 5B), suggesting a negative effect of the phosphorylation. The status of position 114 directly affected the level of the Elp4 protein (Fig. 5C), which is a typical feature of Gsk3-phosphorylated sites (*42*). The effect of mutating S118 was less clear and difficult to interpret, as either alanine or glutamic acid versions behaved closer to the wild type with a clear stabilization of the protein. In addition, the kinase phosphorylating S118 is unknown, and we therefore focused on the S114 site.

We next analyzed the effect of the Elp4 S114A mutation on the TORC1 and TORC2 complexes using the level of phosphorylation of Psk1 (*43*) and Gad8 as specific reporters of the activity of these complexes (Fig. 5D and fig. S7). This experiment revealed that the Elp4 S114A mutation has an opposite effect on TORC1 (Psk1) and TORC2 (Gad8) in favor of TORC2 activity. Similar to a TORC2 mutant, an *elp4* mutant is defective for gametogenesis (Fig. 5E). The defect was complemented by the S114A version of Elp4, confirming the close relationship between Elongator and TORC2. Together, these data suggest that the S114 phosphorylation of Elp4 decreases the activity of Elongator.

We further tested this possibility using LC-MS to measure the impact of the S114 phosphorylation on the subset of Elongator-dependent modifications. The S114A mutation behaved as a deletion mutant of *gsk3*, mostly resulting in an increase of the major Elongator-dependent modified nucleotides (Fig. 6A). A previous study in fission yeast reported that the Ppe1 phosphatase opposes Gsk3 (*44*). We therefore tested the *ppe1* mutant in the same setup, which indicated that it behaved oppositely to Gsk3 and was required for proper level of the Elongator-dependent modifications (Fig. 6A). It will therefore be of interest to test whether Ppe1 can directly dephosphorylate Elp4 when an assay becomes available. To get a condition where rapamycin affects the growth of fission yeast, we combined it with caffeine as previously reported (*45*). Under these conditions, the behavior of the *gsk3* mutants was again opposite to that of the *ppe1* mutant, showing slow growth reminiscent of an *elp4* mutant, while the deletion of *gsk3* suppressed the growth defect of the wild type (Fig. 6B). In addition, the Elp4 S114A mutant substantially suppressed the growth defect of the *ppe1* deletion strain on rapamycin (Fig. 6B).

Together, these data indicate that TORC2 negatively regulates Gsk3 and that, in turn, Gsk3 negatively regulates Elongator through the phosphorylation of Elp4 S114, while Ppe1 likely opposes this phosphorylation. In that context, the structural partner of Ppe1, Ekc1 (*46*), behaved as an activator of Elongator in the genetic screen described in fig. S3. These data also provide a mechanistic view of the role of Elongator in regulating the nutrient-dependent switch between TORC1 and TORC2, as presented in the model shown in fig. S9. To further test this model, we directly analyzed the effect of the deletion of *gsk3* or the inactivation of Elongator on the activities of TORC1 and TORC2 using the phosphorylation of Psk1 and Gad8 as direct specific reporters of TOR signaling (*47*, *48*) (Fig. 6, C and D, fig. S8, and table S2). Within an hour, nitrogen starvation leads to the switch from high TORC1 activity to high TORC2 activity. In the absence of Gsk3, while the inactivation of TORC1 occurred normally, the phosphorylation of Gad8 increased 30 min earlier. The absence of Elp4 led to an opposite effect with persistent TORC1 activity and the inability to activate TORC2. In the reciprocal experiment in which nitrogen is added to starved cells, high TORC2 activity decreased within 30 min, in addition to an increase in TORC1 activity. In the absence of Gsk3, the activation of TORC1 was delayed by about 30 min with persistent TORC2 activity. In the absence of Elongator, TORC1 activity was still detected even during nitrogen starvation and quickly increased when nitrogen was added, while the activity of TORC2 was barely detectable during the entire course of the experiment.

DISCUSSION

This work shows that, by promoting the translation of Tor1 and Ste20 among others, Elongator is a critical activator of the TORC2 complex. In turn, TORC2 releases the inhibitory phosphorylation of Elp4 by Gsk3, therefore creating a positive TORC2-Elongator feedback loop, which is required for the nutrient-dependent control of
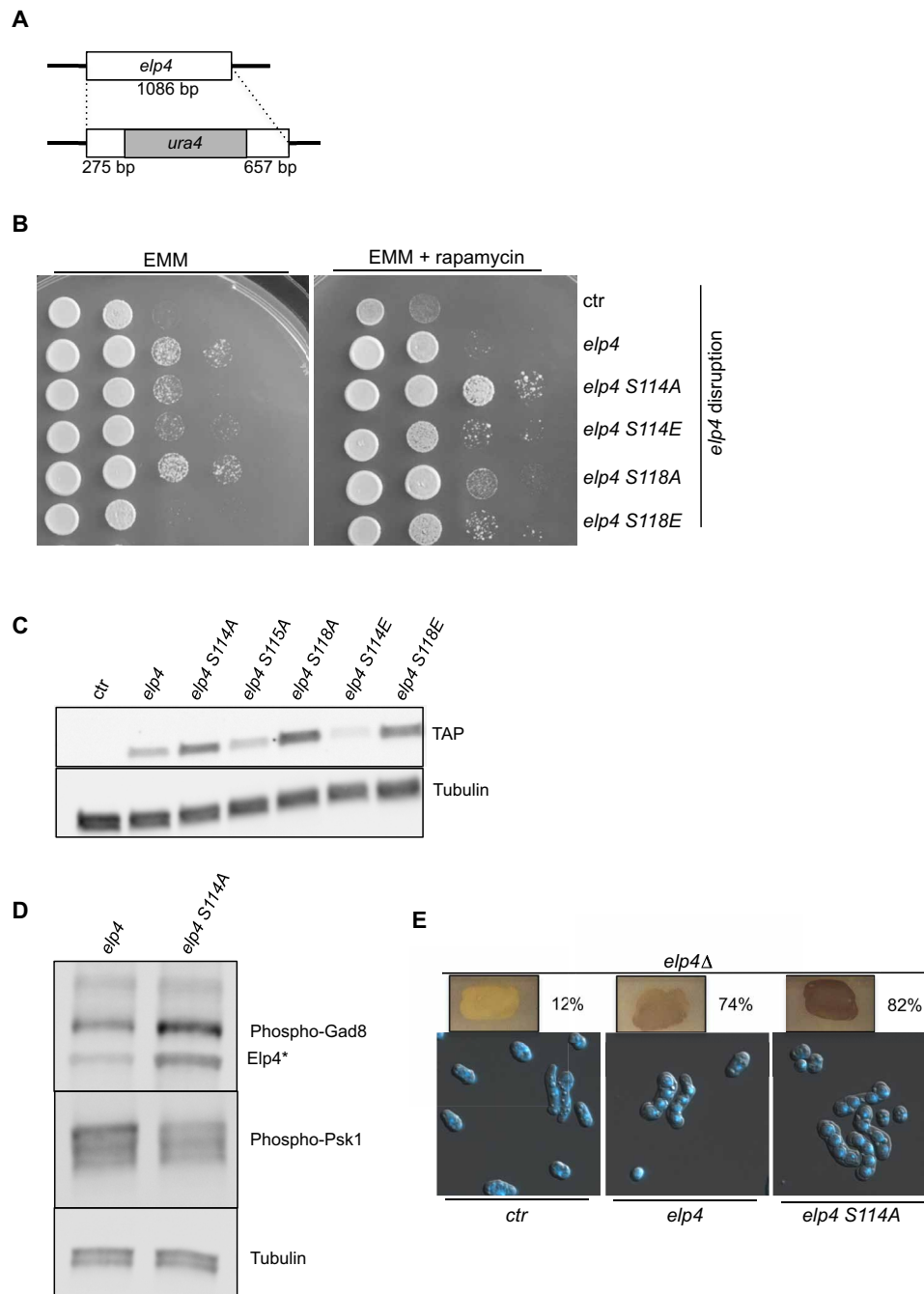
Fig. 5. The S114A mutant is the hyperactive version of Elp4. (**A**) A schematic of the disrupted allele retaining the first 91 amino acids of Elp4. bp, base pair. (**B**) Growth assay of the *elp4* disruption strain transformed with plasmids expressing the indicated wild-type or *elp4* mutants or an empty vector (ctr) in the presence or absence of rapamycin. (**C**) Western blot analysis of the level of expression of the indicated *elp4* mutants. Tubulin is used as a loading control. (**D**) Western blot analyses of the phosphorylation status of Gad8 and Psk1 in a wild-type strain or the Elp4 S114A mutant. Tubulin is used as a loading control. *Note that the anti–phospho-Gad8 antibody also recognizes Elp4 because of the presence of an immunoglobulin G binding domain within the TAP tag. (**E**) Iodine staining and microscopic observations of the sterility in the indicated homothallic *elp4*-deleted strain transformed with plasmids expressing the indicated wild type, *elp4* S114A mutant, or an empty vector (ctr). Clones were grown on low-nitrogen medium for 48 hours. The dark iodine staining indicates the presence of gametes (asci) as confirmed by 4′,6-diamidino-2-phenylindole (DAPI) staining. The mating efficiency is indicated as percentage.

mitosis onset and cell fate (fig. S9). In contrast, Elongator negatively controls TORC1 by sustaining the translation of negative regulators of the complex including the hamartin Tsc1 and Tsc2. Recent work has revealed that the Ppe1-Eck1 phosphatase is inhibited by TORC1

(*49*). Here, we have identified Eck1, an activating subunit of Ppe1, as an activator of Elongator. Together with previous data indicating that Ppe1 counteracts Gsk3 in fission yeast (*44*), the possibility that Ppe1 dephosphorylates Elp4 on S114 exists, therefore creating a
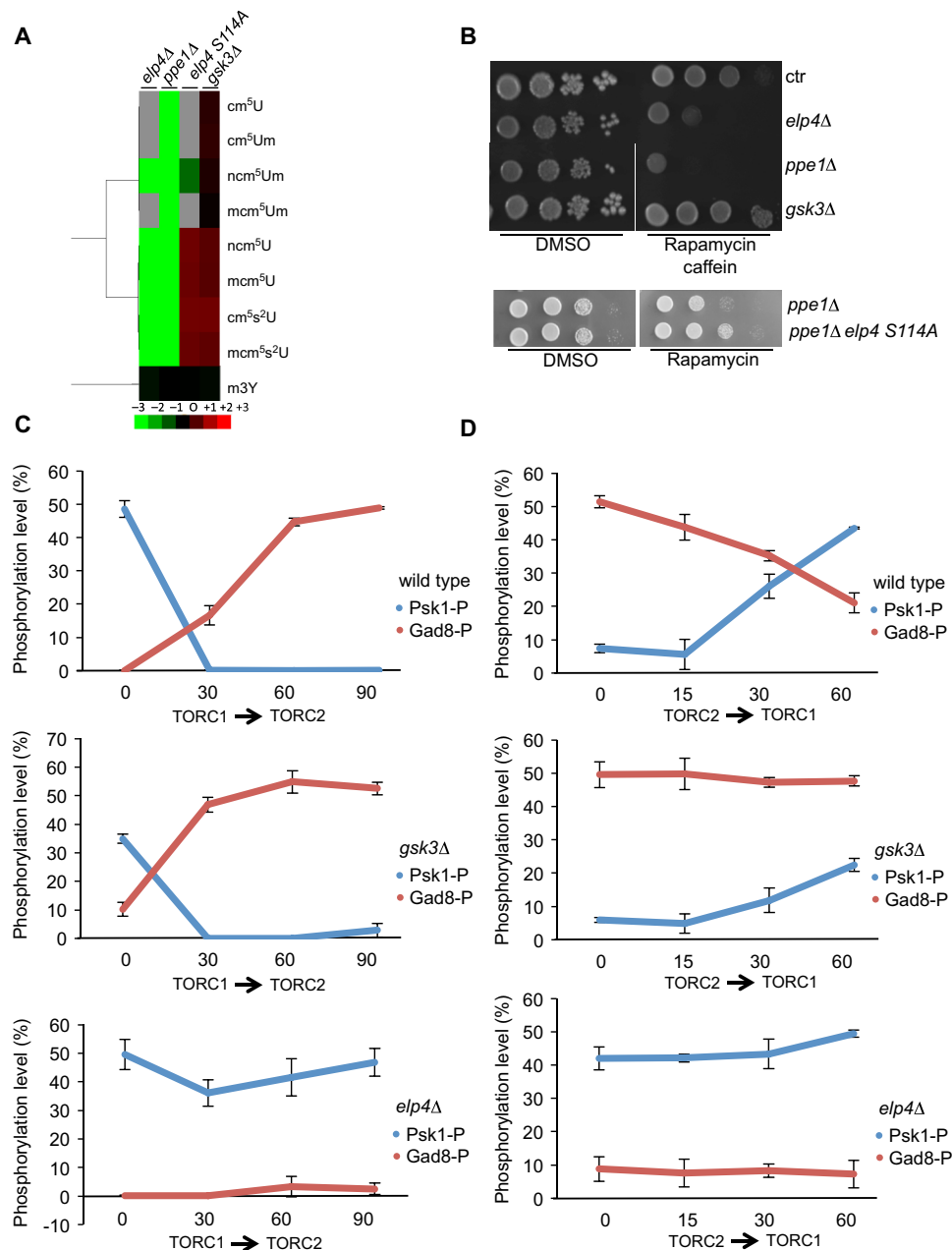
Fig. 6. The balance between TORC1 and TORC2 pathways is regulated by Elongator. (**A**) Cluster analysis visualization of changes in the relative levels of all detectable Elongator-dependent modified ribonucleosides in the indicated strains. The bottom color bar displays the range of log 2 fold change values. (**B**) Growth assay of the indicated strain in the presence of rapamycin/caffeine (top), rapamycin (bottom), or vehicle. DMSO, dimethyl sulfoxide. (**C**) Phosphorylation level of the TORC1 substrate Psk1 and the TORC2 substrate Gad8 during nitrogen starvation. Cells were filtered and resuspended in a medium deprived of nitrogen at time 0 and analyzed for 90 min in the indicated strains. Each point represents the averaged normalized value ± SEM ($n = 3$). (**D**) Phosphorylation level of the TORC1 substrate Psk1 and the TORC2 substrate Gad8 after addition of nitrogen on cells starved for 2 hours. Cells were filtered and resuspended in a medium deprived of nitrogen for 2 hours. Nitrogen (NH_4CL) was added back at time 0, and indicated strains were analyzed for 60 min. Each point represents the averaged normalized value ± SEM ($n = 3$).

negative TORC1-Elongator feedback loop, which we are currently investigating.

The central position of Elongator as a regulator of the balance between TORC1 and TORC2 is also supported genetically. Similar to strains with hyperactive TORC1, Elongator mutants display resistance to canavanine, slow growth when bearing auxotrophic markers, defect in gametogenesis, and the inability to adapt cell size in

response to change in the nitrogen source (*11*). Elongator mutants also share some phenotypes with TORC2 inactivation including moderate cell elongation and misplaced septa (*50*). In addition, it was previously noted on that the levels of Ste20 and Sin1, two components of TORC2, are reduced when the TORC1 kinase Tor2 is overexpressed (*6*), which likely reflects the fact that Elongator is down-regulated under these conditions.

Both TORCs also critically regulate the level of Elongator-dependent tRNA modifications, as shown by MS-based analyses of modified uridine in strains overexpressing either *tor1* or *tor2* (Fig. 4A). Although it was anticipated that Elongator could be regulated on the basis of the phosphorylation of Elp1 (*33*), and despite the requirement of the Hrr25 kinase and the Sit4 phosphatase for the synthesis of the mcm^5 modification (*23*), our work shows that tRNA modification by Elongator not only is a basic requirement for proteome integrity (*51*) but also is regulated by the central growth control machinery of the eukaryotic cell.

The mechanism of the control of Elongator by TORC2 relies on a critical phosphorylation of Elp4, which is regulated by the TORC2-Gad8 branch of the TOR pathway through Gsk3. The site is conserved within the fission yeast clade, and a closely related position was shown to undergo TOR-dependent phosphorylation in the distantly related species *Saccharomyces cerevisiae* (*36*), which suggests that the phosphorylation we report here likely plays a major conserved function. The S114 and flanking consensus are located within a region with overall low conservation that was shown to make intimate contacts with both Elp1 and Elp3 (*52*), which may underlie its importance. Moreover, the fact that two Elp4-Elp5-Elp6 subcomplexes can be loaded onto the Elp1-Elp2-Elp3 two-lobe symmetric scaffold may allow the possibility of double rate synthesis of tRNA modification under some conditions, and the phosphorylation of Elp4 could be critical for this regulation. The Elp4 S114 phosphorylation site is found within a Gsk3 consensus, and our data indeed show that it requires prephosphorylation at the +4 position (S118). In addition, an S114A mutation markedly stabilizes Elp4, which is another well-conserved feature of Gsk3 substrates (*42*). As the phosphorylation of S118 is a prerequisite for efficient S114 phosphorylation, one may anticipate that a S118A mutant would behave similarly to a S114A mutant. However, the S118A mutant rather behaved as the wild type (Fig. 5B). One cannot exclude that S118 phosphorylation has a function on its own, as suggested by the detrimental effect of the S118E mutation, which complicates the interpretation of the behavior of the S118 mutant.

Our data also support that Gsk3 is itself phosphorylated by Gad8, which negatively regulates its activity. This may occur at S335, whose phosphorylation was previously shown to decrease the activity of Gsk3 in fission yeast (*41*). However, this site is not in a perfect Akt-Gad8 consensus, but additional consensus sites, including S282, are present and were not tested here. In addition, the level of Gsk3 phosphorylation by Gad8 in vitro remains weak, which may indicate that the assay is not optimal or that additional kinases function in vivo.

Genome-wide screens for rapamycin sensitivity in fission yeast have shown that the phenotype is not common but specific to Elongator mutants (*53*). Our data show that the sensitivity depends on Tor2, as a *tor2*-resistant allele but not a *tor1*-resistant allele bypasses it. A possibility to explain the sensitivity of Elongator mutant to rapamycin is that, upon addition of the compound, TORC1 activity is decreased but TORC2 cannot be activated because of the low level of Ste20 and Tor1. The resulting uncoordinated TOR activity would be lethal. It was previously reported that a *tor1/tor2* double mutant is not viable despite the opposite functions of both complexes (*11*). Therefore, the concomitant decrease of TORC1 and TORC2 activities when Elongator mutants are grown on rapamycin could similarly result in lethality.

Rapamycin mimics the shortening of the cell cycle that results from a change in the nitrogen source that affects cell fate. The present work shows that Elongator is essential for that process and functions as a central coordinator of the nutrient-dependent control of cell division and cell fate. These findings shed new light on the increasing reports of prominent roles of Elongator in tumorigenesis (*54–56*).

MATERIAL AND METHODS
Fission yeast methods
Wild-type and mutant strains listed in table S4 were grown at 32°C in Edinburgh minimal medium (EMM) with indicated nitrogen source. For starvation, cells were filtered from EMM to the indicated medium using the following nitrogen sources: NH$_4$CL (90 mM), glutamate (20 mM), and proline (10 mM). Rapamycin was used at 25 ng/ml on plates and at 300 ng/ml in liquid cultures. Caffeine was used at 100 μg/ml. Canavanine was used at 75 μg/ml. Fission yeast growth, gene targeting, including locus-specific integration, and mating were performed using classical methods (*57–59*). Western blot was performed with anti-hemagglutinin (HA; H6908, Sigma-Aldrich), peroxidase-antiperoxidase (PAP) (P1291, Sigma-Aldrich), anti-tubulin (T5168, Sigma-Aldrich), anti-Flag (F3165, Sigma-Aldrich), anti-myc (MMS-150P, Covance), anti–phospho–S546-Gad8 (*60*), and anti–phospho-p70 S6 kinase [Phospho-Psk1; 9206, Cell Signaling Technology (*43*)] antibodies. For the secondary screen based on Atf1-HA level, fluorescent Western blotting was performed for normalization using the following antibodies: anti-HA (MMS-101P, Covance), anti-tubulin (T5168, Sigma-Aldrich), and secondary antibody anti-mouse immunoglobulin G IRDye 800CW (610-631-002, Rockland), and each signal was analyzed using LI-COR scanner following the instructions of the manufacturer. Ratio of mutant signal to wild-type signal is calculated. Iodine staining was performed by exposing 48 hours crosses to iodine (*25*).

The deletion of *elp4* in *S. japonicus* was performed by electroporation using a polymerase chain reaction (PCR) product flanked by long homology arms generated by a three-step PCR as previously described (*61*, *62*). Mutageneses were performed using the Q5 Site-Directed Mutagenesis Kit (New England BioLabs). Overexpression of tRNA from plasmids was performed as previously described (*26*). Protein arrays were performed as previously described (*27*). The various versions of *elp4* were expressed from the plasmid pJK148-ars1, including the endogenous *elp4* promoter: pDH731 (*elp4*), pDH733 (*elp4* S114A), pDH735 (*elp4* S118A), pDH749 (*elp4* S114E), pDH776 (*elp4* S118E), and pDH729 (empty vector).

Northern blot
Total RNA was prepared by phenol extraction (*63*) and purified on Qiagen RNeasy. Total RNA (15 to 30 μg) was separated on gel and transferred on nitrocellulose. Hybridization of a multiprime-labeled probe covering indicated positions was performed overnight at 42°C. Quantitative reverse transcription PCR was performed using the ABI High-Capacity RNA-to-cDNA Kit following the instructions of the manufacturer. The untreated sample was used as a reference, and ribosomal RNAs were used as loading controls.

IP-kinase assay
IPs were performed as previously described (*64*): Cells were disrupted with a Fastprep (MP) Biomedicals, and proteins were precipitated on appropriately coated Dynabeads (Invitrogen) following the instructions of the manufacturer for 2 hours and washed four times in NP-40 buffer [6 mM Na$_2$HPO$_4$, 4 mM NaH$_2$PO$_4$, 1% Nonidet P-40,

150 mM NaCl, 2 mM EDTA, and 50 mM NaF supplemented with complete EDTA-free and PhosSTOP tablets (Roche)] and once in kinase buffer [10 mM MgCl$_2$, 50 mM tris-HCl (pH 7.5), 2 mM dithiothreitol, 1 mM EDTA, and 1 mM EGTA] before the kinase reaction in kinase buffer supplemented with 1 μl of γ^{32}P-ATP (adenosine triphosphate; 3000 Ci/mmol), 100 μM ATP, and 1 μg of Elp4 peptide (corresponding to 1 μl). Peptides were synthetized by Eurogentec with the following sequences: Elp4, SAGEDNHSSPPSKN; Elp4, S118-P SAGEDNHSSPPS(Ph)KN; Elp4, S114A S118-P SAGEDNHASPPS(Ph)KN; and Elp4, S115A S118-P SAGEDNHSAPPS (Ph)KN. The assay was performed for 30 min at 30°C and separated on tris-Tricine gel (Bio-Rad). GST-Gsk3 fusion proteins were expressed from pGEX4T1 and purified following the instructions of the manufacturer (GE Healthcare).

Chroma-Glo assay

Yeast were inoculated in 96-well plate in EMM containing amino acids, nucleobases, and thiamine (15 μM) for at least 20 hours before shifting in same medium without thiamine for 16 hours. Thirty microliters of culture was dispatched on a new 96-well plate and mixed with an equal volume of Chroma-Glo reagent. Plate was placed in Berthold and incubated at 30°C for 45 min. Luminescence was measured at 510 and 620 nm. Total luminescence was measured only for experimental tuning because the same filters are used for all screened plates.

Calibration constants were determined by the following measurements of cells expressing only CBR or CBG68, and the Chroma-Luc calculator used to determine corrected luminescence values is available at: www.promega.com: R, total red luminescence measured from CBR without filter; G, total green luminescence measured from CBG68 without filter; Rrf, red luminescence measured from CBR with red filter (610 long-pass filter); Grf, green luminescence measured from CBG68 with red filter (610 long-pass filter); Rgf, red luminescence measured from CBR with green filter (510/60 nm filter); and Ggf, green luminescence measured from CBG68 with green filter (510/60 nm filter). Corrected red luminescence value (R0) and green luminescence value (G0) were determined following the instructions of the manufacturer.

G′ corresponds to the corrected signal of internal standard Ade3-CBG$_{AAG}$, and R′ corresponds to the Elongator-sensitive reporter Cdr2-CBR$_{AAA}$. The R′/G′ ratio is measured for all single-deletion/dual-reporter strains and compared to the wild-type ratio.

Quantification of Psk1 and Gad8 phosphorylation level and statistical analyses

Quantifications were performed by ImageJ on three replicates. Each point represents the averaged normalized value ± SEM ($n = 3$). The raw data and normalizations are presented in table S2. For this experiment (Fig. 6), we preferred to use the myc-tag version rather than the anti–phospho-p70 S6 used in Fig. 5D, which gave more diffused bands.

Quantification of tRNA modifications

Modified ribonucleosides in tRNA were identified and quantified, as previously reported (34, 65, 66). Total RNAs were extracted and enriched in small RNAs (<200 nt, >85% tRNA) using the PureLink miRNA Isolation Kit (Invitrogen). The quantity of tRNA was then determined by ultraviolet spectrophotometer at 260 nm and Agilent Bioanalyzer analysis (small RNA kit). Using identical quantities of tRNA from various strains, each sample was mixed with (^{15}N)$_5$-2-deoxyadenosine as internal standard, and the tRNAs were enzymatically hydrolyzed using 1 μg of coformycin, 4 mM butylated hydroxytoluene, 5 μg of tetrahydrouridine, 8.5 mM MgCl$_2$, 85 mM tris (pH 7.9), 25 U of Benzonase, 0.2 U of phosphodiesterase, and 5 U of alkaline phosphatase and incubated at 37°C for 3 hours. The enzymes and other large molecules were removed by ultrafiltration.

The digested ribonucleosides were resolved on a Thermo Hypersil GOLD aQ column (100 mm by 2.1 mm; particle size, 1.9 μm) in a two-buffer eluent system, with buffer A consisting of water with 0.1% (v/v) formic acid and buffer B consisting of acetonitrile with 0.1% (v/v) formic acid. High-performance liquid chromatography (HPLC) was performed at a flow rate of 0.3 ml/min. The gradient of acetonitrile in 0.1% formic acid was as follows: 0 to 12 min, held at 0%; 12 to 15.3 min, 0 to 1%; 15.3 to 18.7 min, 1 to 6%; 18.7 to 20 min, 6%; 20 to 24 min, 6 to 100%; 24 to 27.3 min, 100%; 27.3 to 28 min, 100 to 0%; and 28 to 41 min, 0%. The HPLC column was maintained at 25°C and directly connected to an Agilent 6490 triple quadrupole ion funnel mass spectrometer (LC–tandem MS) with ESI Jet Stream ionization operated in positive ion mode. Modified ribonucleosides were identified by HPLC retention time and collision-induced dissociation fragmentation pattern. Multiple reaction monitoring was performed to detect and quantify the ribonucleosides with the parameters of retention time, mass/charge ratio (m/z) of the transmitted parent ion, and m/z of the monitored product ion and dwell time, as noted below. Collision energies and cell accelerator voltages were optimized on the basis of commercial standards. The fragmentor voltage was fixed at 380 V, with MS1 and MS2 filters set at unit resolution. The voltages and source parameters were as follows: gas temperature, 50°C; gas flow, 11 liters/min; nebulizer, 20 psi; sheath gas temperature, 300°C; sheath gas flow, 12 liters/min; capillary voltage, 1800 V; and charging voltage 2000 V.

The signal intensity for each ribonucleoside was normalized with the signal intensity of the spike-in standard, and abundance of the modified ribonucleosides was compared to the control. The spike-in standard and canonical ribonucleosides (A, U, G, and C) varied between 7 and 17% across all samples, suggesting that run-to-run variation due to sample handling and day-to-day machine fluctuation were kept to a minimum. The raw data used to generate the clusters shown in Figs. 4A and 6A are presented in table S3.

SUPPLEMENTARY MATERIALS

Table S3. Raw and processed data of the quantification of tRNA modifications used to build Figure 3A, left (sheet 1), 3A, right (sheet 2), and 4A (sheet 3).

Table S4. List of strains used and generated in this study.

REFERENCES AND NOTES

1. I. J. McDonald, G. B. Callejam, B. F. Johnson, Conjugation in chemostat cultures of *Schizosaccharomyces pombe*. *J. Gen. Microbiol.* **128**, 1981–1987 (1982).

2. R. Egel, Commitment to meiosis in fission yeast. *Mol. Gen. Genet.* **121**, 277–284 (1973).

3. D.-H. Kim, D. D. Sarbassov, S. M. Ali, J. E. King, R. R. Latek, H. Erdjument-Bromage, P. Tempst, D. M. Sabatini, mTOR interacts with raptor to form a nutrient-sensitive complex that signals to the cell growth machinery. *Cell* **110**, 163–175 (2002).

4. J. Montagne, M. J. Stewart, H. Stocker, E. Hafen, S. C. Kozma, G. Thomas, *Drosophila* S6 kinase: A regulator of cell size. *Science* **285**, 2126–2129 (1999).

5. B. Álvarez, S. Moreno, Fission yeast Tor2 promotes cell growth and represses cell differentiation. *J. Cell Sci.* **119**, 4475–4485 (2006).

6. T. Matsuo, Y. Otsubo, J. Urano, F. Tamanoi, M. Yamamoto, Loss of the TOR kinase Tor2 mimics nitrogen starvation and activates the sexual development pathway in fission yeast. *Mol. Cell. Biol.* **27**, 3154–3164 (2007).

7. Y. Otsubo, M. Yamamato, TOR signaling in fission yeast. *Crit. Rev. Biochem. Mol. Biol.* **43**, 277–283 (2008).

8. J. Kanoh, M. Yanagida, Chapter 14—Structure of TOR complexes in fission yeast. *Enzymes* **27**, 271–283 (2010).

9. R. Weisman, Target of rapamycin (TOR) regulates growth in response to nutritional signals. *Microbiol. Spectr.* **4**, 10.1128/microbiolspec.FUNK-0006-2016 (2016).

10. Y. Otsubo, M. Yamamoto, in *The Enzymes* (Elsevier, 2010), pp. 229–249, vol. 27.

11. R. Weisman, Fission yeast TOR and rapamycin. *Enzymes* **27**, 251–268 (2010).

12. R. Weisman, I. Roitburg, M. Schonbrun, R. Harari, M. Kupiec, Opposite effects of Tor1 and Tor2 on nitrogen starvation responses in fission yeast. *Genetics* **175**, 1153–1162 (2007).

13. R. Martin, M. Portantier, N. Chica, M. Nyquist-Andersen, J. Mata, S. Lopez-Aviles, A PP2A-B55-mediated crosstalk between TORC1 and TORC2 regulates the differentiation response in fission yeast. *Curr. Biol.* **27**, 175–188 (2017).

14. N. Chica, A. E. Rozalén, L. Pérez-Hidalgo, A. Rubio, B. Novak, S. Moreno, Nutritional control of cell size by the greatwall-endosulfine-PP2A.B55 pathway. *Curr. Biol.* **26**, 319–330 (2016).

15. P. F. Agris, F. A. P. Vendeix, W. D. Graham, tRNA's wobble decoding of the genome: 40 years of modification. *J. Mol. Biol.* **366**, 1–13 (2007).

16. G. R. Björk, *tRNA: Structure, Biosynthesis, and Function*, D. Söll, U. RajBhandary, Eds. (American Society for Microbiology, 1995), pp. 165–205, vol. 11.

17. T. Suzuki, Topics in current genetics, in *Fine-Tuning of RNA Functions by Modification and Editing*, H. Grosjean, Ed. (Springer-Verlag, 2005), vol. 12.

18. M. K. Krüger, S. Pedersen, T. G. Hagervall, M. A. Sørensen, The modification of the wobble base of tRNA^{Glu} modulates the translation rate of glutamic acid codons in vivo. *J. Mol. Biol.* **284**, 621–631 (1998).

19. F. V. Murphy IV, V. Ramakrishnan, A. Malkiewicz, P. F. Agris, The role of modifications in codon discrimination by tRNA$^{Lys}_{UUU}$. *Nat. Struct. Mol. Biol.* **11**, 1186–1191 (2004).

20. C. Yarian, M. Marszalek, E. Sochacka, A. Malkiewicz, R. Guenther, A. Miskiewicz, P. F. Agris, Modified nucleoside dependent Watson-Crick and wobble codon binding by tRNA$^{Lys}_{UUU}$ species. *Biochemistry* **39**, 13390–13395 (2000).

21. A. Esberg, B. Huang, M. J. O. Johansson, A. S. Byström, Elevated levels of two tRNA species bypass the requirement for elongator complex in transcription and exocytosis. *Mol. Cell* **24**, 139–148 (2006).

22. B. Huang, M. J. O. Johansson, A. S. Byström, An early step in wobble uridine tRNA modification requires the Elongator complex. *RNA* **11**, 424–436 (2005).

23. B. Huang, J. Lu, A. S. Byström, A genome-wide screen identifies genes required for formation of the wobble nucleoside 5-methoxycarbonylmethyl-2-thiouridine in *Saccharomyces cerevisiae*. *RNA* **14**, 2183–2194 (2008).

24. O. Kolaj-Robin, B. Séraphin, Structures and activities of the elongator complex and its cofactors. *Enzyme* **41**, 117–149 (2017).

25. F. Bauer, D. Hermand, A coordinated codon-dependent regulation of translation by Elongator. *Cell Cycle* **11**, 4524–4529 (2012).

26. F. Bauer, A. Matsuyama, J. Candiracci, M. Dieu, J. Scheliga, D. A. Wolf, M. Yoshida, D. Hermand, Translational control of cell division by Elongator. *Cell Rep.* **1**, 424–433 (2012).

27. F. Bauer, A. Matsuyama, M. Yoshida, D. Hermand, Determining proteome-wide expression levels using reverse protein arrays in fission yeast. *Nat. Protoc.* **7**, 1830–1835 (2012).

28. E. Davie, J. Petersen, Environmental control of cell size at division. *Curr. Opin. Cell Biol.* **24**, 838–844 (2012).

29. J. Petersen, TOR signalling regulates mitotic commitment through stress-activated MAPK and Polo kinase in response to nutrient stress. *Biochem. Soc. Trans.* **37**, 273–277 (2009).

30. J. Petersen, P. Nurse, TOR signalling regulates mitotic commitment through the stress MAP kinase pathway and the Polo and Cdc2 kinases. *Nat. Cell Biol.* **9**, 1263–1272 (2007).

31. Y. Shimada, M. Bühler, *Schizosaccharomyces pombe* reporter strains for relative quantitative assessment of heterochromatin silencing. *Yeast* **29**, 335–341 (2012).

32. J. Fernandez-Vazquez, I. Vargas-Pérez, M. Sansó, K. Buhne, M. Carmona, E. Paulo, D. Hermand, M. Rodríguez-Gabriel, J. Ayté, S. Leidel, E. Hidalgo, Modification of tRNA$^{Lys}_{UUU}$ by elongator is essential for efficient translation of stress mRNAs. *PLOS Genet.* **9**, e1003647 (2013).

33. W. Abdel-Fattah, D. Jablonowski, R. di Santo, K. L. Thüring, V. Scheidt, A. Hammermeister, S. ten Have, M. Helm, R. Schaffrath, M. J. R. Stark, Phosphorylation of Elp1 by Hrr25 is required for elongator-dependent tRNA modification in yeast. *PLOS Genet.* **11**, e1004931 (2015).

34. C. T. Y. Chan, M. Dyavaiah, M. S. DeMott, K. Taghizadeh, P. C. Dedon, T. J. Begley, A quantitative systems approach reveals dynamic control of tRNA modifications during cellular stress. *PLOS Genet.* **6**, e1001247 (2010).

35. M. Dewez, F. Bauer, M. Dieu, M. Raes, J. Vandenhaute, D. Hermand, The conserved Wobble uridine tRNA thiolase Ctu1-Ctu2 is required to maintain genome integrity. *Proc. Natl. Acad. Sci. U.S.A.* **105**, 5459–5464 (2008).

36. A. Soulard, A. Cremonesi, S. Moes, F. Schütz, P. Jenö, M. N. Hall, The rapamycin-sensitive phosphoproteome reveals that TOR controls protein kinase A toward some but not all substrates. *Mol. Biol. Cell* **21**, 3475–3486 (2010).

37. A. Carpy, K. Krug, S. Graf, A. Koch, S. Popic, S. Hauf, B. Macek, Absolute proteome and phosphoproteome dynamics during the cell cycle of *Schizosaccharomyces pombe* (Fission Yeast). *Mol. Cell. Proteomics* **13**, 1925–1936 (2014).

38. A. Koch, K. Krug, S. Pengelley, B. Macek, S. Hauf, Mitotic substrates of the kinase aurora with roles in chromatin regulation identified through quantitative phosphoproteomics of fission yeast. *Sci. Signal.* **4**, rs6 (2011).

39. F. Vigneron, P. Dos Santos, S. Lemoine, M. Bonnet, L. Tariosse, T. Couffinhal, C. Duplaà, B. Jaspard-Vinassa, GSK-3β at the crossroads in the signalling of heart preconditioning: Implication of mTOR and Wnt pathways. *Cardiovasc. Res.* **90**, 49–56 (2011).

40. J. Dal Col, R. Dolcetti, GSK-3b inhibition: At the crossroad between Akt and mTOR constitutive activation to enhance cyclin D1 protein stability in mantle cell lymphoma. *Cell Cycle* **7**, 2813–2816 (2008).

41. S. E. Plyte, A. Feoktistova, J. D. Burke, J. R. Woodgett, K. L. Gould, *Schizosaccharomyces pombe* skp1+ encodes a protein kinase related to mammalian glycogen synthase kinase 3 and complements a cdc14 cytokinesis mutant. *Mol. Cell. Biol.* **16**, 179–191 (1996).

42. M. A. Hermida, J. Dinesh Kumar, N. R. Leslie, GSK3 and its interactions with the PI3K/AKT/mTOR signalling network. *Adv. Biol. Regul.* **65**, 5–15 (2017).

43. Y. Otsubo, T. Matsuo, A. Nishimura, M. Yamamoto, A. Yamashita, tRNA production links nutrient conditions to the onset of sexual differentiation through the TORC1 pathway. *EMBO Rep.* **19**, e44867 (2018).

44. G. Goshima, O. Iwasaki, C. Obuse, M. Yanagida, The role of Ppe1/PP6 phosphatase for equal chromosome segregation in fission yeast kinetochore. *EMBO J.* **22**, 2752–2763 (2003).

45. C. Rallis, S. Codlin, J. Bähler, TORC1 signaling inhibition by rapamycin and caffeine affect lifespan, global gene expression, and cell proliferation of fission yeast. *Aging Cell* **12**, 563–573 (2013).

46. M. Yanagida, N. Ikai, M. Shimanuki, K. Sajiki, Nutrient limitations alter cell division control and chromosome segregation through growth-related kinases and phosphatases. *Philos. Trans. R. Soc. Lond. B Biol. Sci.* **366**, 3508–3520 (2011).

47. Y. Otsubo, A. Nakashima, M. Yamamoto, A. Yamashita, TORC1-dependent phosphorylation targets in fission yeast. *Biomol. Ther.* **7**, E50 (2017).

48. T. Matsuo, Y. Kubo, Y. Watanabe, M. Yamamoto, *Schizosaccharomyces pombe* AGC family kinase Gad8p forms a conserved signaling module with TOR and PDK1-like kinases. *EMBO J.* **22**, 3073–3083 (2003).

49. D. Laor, A. Cohen, M. Kupiec, R. Weisman, TORC1 regulates developmental responses to nitrogen stress via regulation of the GATA transcription factor Gaf1. *MBio* **6**, e00959 (2015).

50. N. Ikai, N. Nakazawa, T. Hayashi, M. Yanagida, The reverse, but coordinated, roles of Tor2 (TORC1) and Tor1 (TORC2) kinases for growth, cell cycle and separase-mediated mitosis in *Schizosaccharomyces pombe*. *Open Biol.* **1**, 110007 (2011).

51. D. D. Nedialkova, S. A. Leidel, Optimization of codon translation rates via tRNA modifications maintains proteome integrity. *Cell* **161**, 1606–1618 (2015).

52. M. I. Dauden, J. Kosinski, O. Kolaj-Robin, A. Desfosses, A. Ori, C. Faux, N. A. Hoffmann, O. F. Onuma, K. D. Breunig, M. Beck, C. Sachse, B. Séraphin, S. Glatt, C. W. Müller, Architecture of the yeast Elongator complex. *EMBO Rep.* **18**, 264–279 (2017).

53. A. Doi, A. Fujimoto, S. Sato, T. Uno, Y. Kanda, K. Asami, Y. Tanaka, A. Kita, R. Satoh, R. Sugiura, Chemical genomics approach to identify genes associated with sensitivity to rapamycin in the fission yeast *Schizosaccharomyces pombe*. *Genes Cells* **20**, 292–309 (2015).

54. A. Ladang, F. Rapino, L. C. Heukamp, L. Tharun, K. Shostak, D. Hermand, S. Delaunay, I. Kleveric, Z. Jiang, N. Jacques, D. Jamart, V. Migeot, A. Florin, S. Göktuna, B. Malgrange, O. J. Sansom, L. Nguyen, R. Büttner, P. Close, A. Chariot, Elp3 drives Wnt-dependent tumor initiation and regeneration in the intestine. *J. Exp. Med.* **212**, 2057–2075 (2015).

55. P. Close, M. Gillard, A. Ladang, Z. Jiang, J. Papuga, N. Hawkes, L. Nguyen, J.-P. Chapelle, F. Bouillenne, J. Svejstrup, M. Fillet, A. Chariot, DERP6 (ELP5) and C3ORF75 (ELP6) regulate tumorigenicity and migration of melanoma cells as subunits of Elongator. *J. Biol. Chem.* **287**, 32535–32545 (2012).

56. F. Rapino, S. Delaunay, F. Rambow, Z. Zhou, L. Tharun, P. de Tullio, O. Sin, K. Shostak, S. Schmitz, J. Piepers, B. Ghesquière, L. Karim, B. Charloteaux, D. Jamart, A. Florin, C. Lambert, A. Rorive, G. Jerusalem, E. Leucci, M. Dewaele, M. Vooijs, S. A. Leidel, M. Georges, M. Voz, B. Peers, R. Büttner, J.-C. Marine, A. Chariot, P. Close, Codon-specific translation reprogramming promotes resistance to targeted therapy. *Nature* **558**, 605–609 (2018).

57. S. Bamps, T. Westerling, A. Pihlak, L. Tafforeau, J. Vandenhaute, T. P. Mäkelä, D. Hermand, Mcs2 and a novel CAK subunit Pmh1 associate with Skp1 in fission yeast. *Biochem. Biophys. Res. Commun.* **325**, 1424–1432 (2004).

58. M. Devos, E. Mommaerts, V. Migeot, H. van Bakel, D. Hermand, Fission yeast Cdk7 controls gene expression through both its CAK and C-terminal domain kinase activities. *Mol. Cell. Biol.* **35**, 1480–1490 (2015).

59. N. Fersht, D. Hermand, J. Hayles, P. Nurse, Cdc18/CDC6 activates the Rad3-dependent checkpoint in the fission yeast. *Nucleic Acids Res.* **35**, 5323–5337 (2007).

60. H. Nurse, S. Morigasaki, S. Murayama, C. T. Zeng, K. Shiozaki, Rab-family GTPase regulates TOR complex 2 signaling in fission yeast. *Curr. Biol.* **20**, 1975–1982 (2010).

61. S. Nozaki, K. Furuya, H. Niki, The Ras1-Cdc42 pathway is involved in hyphal development of *Schizosaccharomyces japonicus*. *FEMS Yeast Res.* **18**, foy031 (2018).

62. K. Aoki, K. Furuya, H. Niki, Transformation of *Schizosaccharomyces japonicus*. *Cold Spring Harb. Protoc.* **2017**, pdb.prot091850 (2017).

63. A. Guiguen, J. Soutourina, M. Dewez, L. Tafforeau, M. Dieu, M. Raes, J. Vandenhaute, M. Werner, D. Hermand, Recruitment of P-TEFb (Cdk9-Pch1) to chromatin by the cap-methyl transferase Pcm1 in fission yeast. *EMBO J.* **26**, 1552–1559 (2007).

64. D. Hermand, A. Pihlak, T. Westerling, V. Damagnez, J. Vandenhaute, G. Cottarel, T. P. Mäkelä, Fission yeast Csk1 is a CAK-activating kinase (CAKAK). *EMBO J.* **17**, 7230–7238 (1998).

65. W. Deng, I. R. Babu, D. Su, S. Yin, T. J. Begley, P. C. Dedon, Trm9-catalyzed tRNA modifications regulate global protein expression by codon-biased translation. *PLOS Genet.* **11**, e1005706 (2015).

66. C. T. Y. Chan, Y. L. J. Pang, W. Deng, I. R. Babu, M. Dyavaiah, T. J. Begley, P. C. Dedon, Reprogramming of tRNA modifications controls the oxidative stress response by codon-biased translation of proteins. *Nat. Commun.* **3**, 937 (2012).

Citation: J. Candiracci, V. Migeot, Y.-H. Chionh, F. Bauer, T. Brochier, B. Russell, K. Shiozaki, P. Dedon, D. Hermand, Reciprocal regulation of TORC signaling and tRNA modifications by Elongator enforces nutrient-dependent cell fate. *Sci. Adv.* **5**, eaav0184 (2019).